Graphene Integrated Silicon Photonics

R. Kou [1,2,3], S. Tanabe [4], T. Tsuchizawa [1,2], K. Warabi [3], Y. Kobayashi [3], S. Suzuki [4],
H. Hibino [4], T. Yamamoto [2], H. Nakajima [3], K. Yamada [1,2]

[1]*NTT Nanophotonics Center, 3-1, Morinosato Wakamiya, Atsugi, Kanagawa 243-0198, Japan*
[2]*NTT Microsystem Integration Laboratories, 3-1, Morinosato Wakamiya, Atsugi, Kanagawa 243-0198, Japan*
[3]*Gradutate School of Advanced Science and Engineering, Waseda University. 3-4-1, Okubo, Shinjuku-ku, Tokyo 169-8555, Japan*
[4]*NTT Basic Research Laboratories, 3-1, Morinosato Wakamiya, Atsugi, Kanagawa 243-0198, Japan*
takahashi.rai@lab.ntt.co.jp

Abstract: We have investigated light-matter interactions in monolayer graphene integration on a silicon-photonic waveguide in telecommunications bands of 1.5 μm. The passive integration scheme and device characteristics are discussed with our recent experimental results and analysis.

1. Introduction

Devices based on silicon photonics technologies provide various advantages in optical communications systems. Except for a monolithic light source, those devices have been comprehensively developed over the last ten years [1]. The next step for enhancing device integration density and operation bandwidth, reducing cost and power consumption requires innovative approaches. Here, we propose the use of graphene, which is composed of carbon-atoms with honeycomb structure. The unique linear energy dispersion in grapheme (Fig. 1) provides remarkable optical features, such as wavelength-independent light absorption (2.3 %/layer), ultrahigh carrier mobility (10^6 cm^2/Vs), a saturable absorption effect, and a tunable Fermi level and band gap (with bilayer graphene). These features would contribute to overcoming the limitations of silicon photonic devices. In this paper, we describe how we apply existing silicon photonics technologies as an integration platform to maximize graphene's potential for achieving future ultrahigh performance opto-electro integrated circuits.

2. Device design and integration process

Fig. 2(a) shows the target structure for monolayer graphene integration on a silicon-photonic waveguide. Thanks for the large evanescent field surrounding the silicon waveguide core, the interaction between light and grapheme is very strong as shown in Fig. 2(b), which corresponds to the propagation mode profile for TE polarization. To realize this basic structure, we developed the integration process briefly summarized in Fig. 3. Large-scale monolayer graphene (50×50 mm^2) grown on copper foil by the CVD method is transferred onto a 4-inch as-etched silicon waveguide SOI wafer. Then, we define graphene patterns using photolithography and O_2 plasma etching. This process enables us to obtain a high-resolution and a flexible shape in graphene.

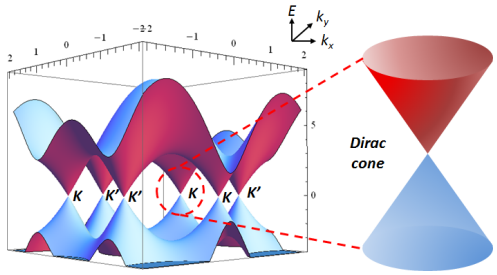

Fig. 1. Energy dispersion in graphene

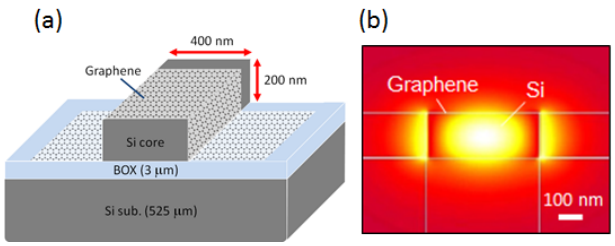

Fig. 2. (a) Schematic of graphene integration on silicon waveguide (b) Calculated mode profile with graphene

3. Device characterization

Fig. 4 shows optical microscope and SEM images of the integration, and micro-Raman spectra from the circled areas in the images. The graphene integrated part (circle 1) has the obvious inherent

response of monolayer graphene. In the optical measurement, we first investigated the light-absorption efficiency of the graphene on a silicon waveguide, and polarization dependence by changing the integrated graphene length from 2.5 to 200 μm. The measured efficiencies were 0.09 dB/μm in the TE mode, and 0.05 dB/μm in the TM mode. From measurement results and numerical analysis, we found that the lower absorption efficiency in the TM mode is due to strong p-doing in the transferred graphene. The p-doping causes surface-plasmon polariton propagation, which results in the low-loss propagation [2]. Next, we investigated the influence of graphene on the resonance Q factor variation by integrating graphene on a silicon-ring resonator. Fig. 5(a) shows a schematic of the sample, where parameter $L_{Gr.}$ corresponds to graphene length from 0 to 20 μm. As shown in Fig. 5(b), the initial Q factor of 7900 drastically decreased to 1200 at $L_{Gr.}$ of 20 μm [3]. We analysed this phenomenon by mode calculation and theoretical approaches and then found that it can be explained by linear graphene absorption on the silicon waveguide. Currently, the only remaining issue for forming passive graphene integrated devices is fiber coupling. Since graphene is a single-atomic-layer material, damage caused by the upper over-cladding layer is very serious. We recently proposed the use of an efficient (1.4 and 2.4 dB/facet in the TE and TM modes) and ultra-broadband (> 300 nm at 3-dB roll off in the both polarizations) selective spot-size converter as a way to solve the problem [4].

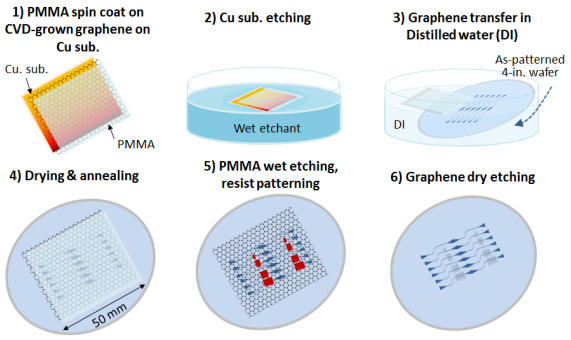

Fig. 3. Fabrication process flow for integration of graphene and silicon photonics

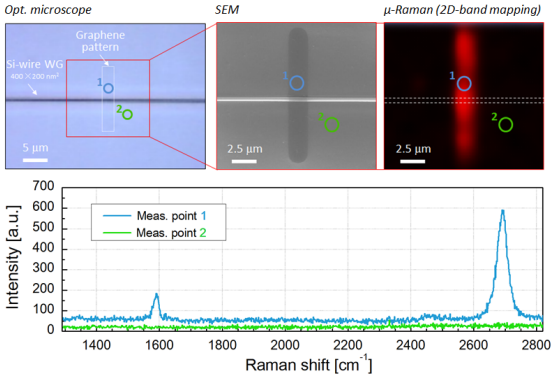

Fig. 4. Optical microscope and SEM images of integration, and micro-Raman spectra. The spectra correspond to each measurement point.

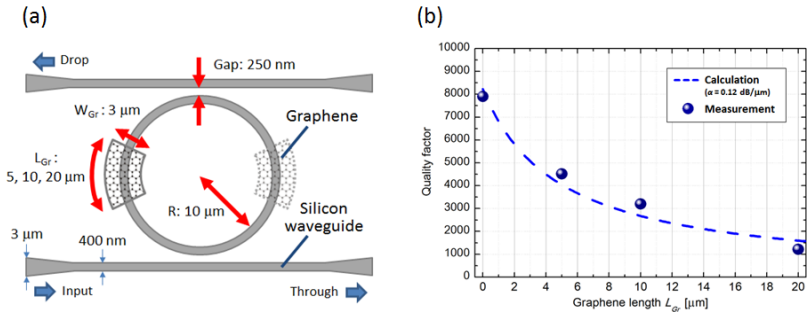

Fig. 5 (a) Partial graphene integration on a silicon ring-resonator. (b) Q factor variation by changing graphene length.

4. Conclusion

We introduced our recent activities on passive graphene integration with silicon-photonic circuits, such as a simple straight waveguide, ring resonator, and selectively spot-size converter. Our results will contribute to the development of large-scale and high-performance circuits using group-IV materials of silicon and graphene in the near future.

References

1. B. Analui, D. Guckenberger, D. Kucharski et al. *IEEE J. Solid-State Circuits* **41**, 12, pp. 2945-2955 (2006).
2. R. Kou, S. Tanabe, T. Tsuchizawa et al. *Jpn. J. Appl. Phys.* **52**, 6, 060203 (2013).
3. R. Kou, S. Tanabe, T. Tsuchizawa et al. *Appl. Phys. Lett.* **104**, 9, 091122 (2014).
4. R. Kou, Y. Kobayashi, K. Warabi et al. *IEEE Photon. J.* **6**, 3, 6600409 (2014).